

This article appeared in a journal published by Elsevier. The attached copy is furnished to the author for internal non-commercial research and education use, including for instruction at the authors institution and sharing with colleagues.

Other uses, including reproduction and distribution, or selling or licensing copies, or posting to personal, institutional or third party websites are prohibited.

In most cases authors are permitted to post their version of the article (e.g. in Word or Tex form) to their personal website or institutional repository. Authors requiring further information regarding Elsevier's archiving and manuscript policies are encouraged to visit:

<http://www.elsevier.com/copyright>



Contents lists available at SciVerse ScienceDirect

## Chemical Physics Letters

journal homepage: [www.elsevier.com/locate/cplett](http://www.elsevier.com/locate/cplett)

## Wavelength-dependent metal-enhanced fluorescence using synchronous spectral analysis

Anatoliy I. Dragan, Buddha Mali, Chris D. Geddes\*

Institute of Fluorescence and Department of Chemistry and Biochemistry, UMBC, 701 East Pratt Street, Baltimore, MD 21202, USA

## ARTICLE INFO

## Article history:

Received 1 August 2012

In final form 17 November 2012

Available online 27 November 2012

## ABSTRACT

The fluorescence spectrum of Au-clusters (8- and 25-atom), which covers the spectral range 350–900 nm, is dramatically enhanced in the presence of plasmon supporting plate-well deposited nanoparticles. The wavelength-dependent metal-enhanced fluorescence (MEF spectrum) correlates well with the plasmon specific scattering spectrum, i.e. the synchronous scatter spectrum of the silver surface of plate wells. Our findings suggest that the synchronous scatter spectra of plasmon enhancing substrates is a good indicator of both the magnitude and the wavelength-dependence of MEF.

© 2012 Elsevier B.V. All rights reserved.

## 1. Introduction

Fluorescence spectroscopy is a powerful tool for the detection of biomolecules (proteins and nucleic acids), studying their interaction with partners and the visualization of macromolecular complexes and cell organelles [1,2]. At the base of these applications is a vast quantity of different fluorescent chromophores, which can be used in different spectral regions, from the UV to NIR. Despite a vast amount of available fluorophores, there is still great demand for probes which are extremely bright and photostable and, subsequently, one's which are able to significantly increase the sensitivity of various detection approaches, including methods such as single-molecule detection and fluorescence correlation spectroscopy [1,3,4]. Modern chromophores, have been specifically synthesized for these purposes, e.g. the Alexa dyes for labeling protein and nucleic acids have large brightness,  $>100000 \text{ M}^{-1} \text{ cm}^{-1}$ , and enhanced photostability.

In recent years the metal-enhanced fluorescence (MEF) phenomenon, which dramatically enhances the brightness of chromophores and, at the same time, increases their photostability, has remarkably improved and broadened fluorescence-based applications in the lifesciences [5–8]. While the MEF phenomenon has been well-studied over the last decade, there are still numerous questions unanswered. Our laboratory has contributed significantly to developing the MEF approach and understanding the mechanisms of metal-enhanced fluorescence [5,6,9,10]. At the heart of the MEF phenomenon lies the interaction between the

*Abbreviations:* NC, nanocluster; NP, nanoparticle; BSA, bovine serum albumin; ANS, 1-anilino-8-naphthalene sulfonate; Au(8), 8-atom gold cluster; Au(25), 25-atom gold cluster; MEF, metal-enhanced fluorescence.

\* Corresponding author. Fax: +1 410 576 5722.

E-mail addresses: [geddes@umbc.edu](mailto:geddes@umbc.edu), [iof@umbc.edu](mailto:iof@umbc.edu) (C.D. Geddes).

electronic states of chromophores and the near-field, generated around nanoparticles (NPs), and the effective coupling between them occurring at a short ( $<50 \text{ nm}$ ) dye-NP distance. Originally, the origin of dye-NP coupling and enhancement of fluorescence was explained by a change in the radiative decay rate of a chromophore, which affords for higher fluorophore quantum yields and a reduced fluorophore lifetime (decay time) [1,11,12]. Subsequently one was previously able to make several conclusions: (1) MEF depends on the free-space quantum yield of a chromophore, i.e. MEF is larger for dyes with a low quantum yield; (2) MEF does not depend on wavelength, as the dye alone radiates the light and the wavelength distribution of the energy is determined solely by inner properties of the chromophore electronic system, and its interactions with the solvent. However, recent experimental works have shown that the interactions in dye-NP systems are significantly more complex than a simple radiative rate mechanism. In particular, it has recently been shown that the far-field fluorophore quantum yield,  $Q_0$ , has little relationship to fluorescence enhancement factors in MEF [10]. In addition, a wavelength dependence has been shown for Prodan in different solvents [13].

In recent years Geddes and colleagues have shown that the mechanisms of metal enhancement can be considered as due to at least two complementary effects: an enhanced absorption and an enhanced emission component [5,10]. According to this interpretation the enhanced absorption in MEF is facilitated by the electric field generated by NPs, its intensity and spectral distribution. Nanoparticle free oscillating electrons (plasmons) have specific absorption and scattering bands [5,6]. The plasmon scattering component is sensitive to the size, shape and density of nanoparticles, and typically increases and broadens (red shift) with NP size. For silver NP films we have found that the plasmon scattering spectra can be directly measured using the synchronous mode of spectral collection. Knowledge of the plasmon scattering characteristics

of silver films gives an opportunity to address some key questions regarding the mechanisms of MEF, for example: does MEF wavelength dependence follow the plasmon scattering spectra? Is there a dependence of the magnitude of MEF upon the incident light wavelength?

To subsequently address these questions we have used fluorescent Au-clusters, an emerging new class of the chromophores, since their spectral properties, specifically their broad emission and absorption spectrum, can be used to study MEF over a broad wavelength range.

## 2. Materials and methods

Chloroauric acid ( $\text{HAuCl}_4$ ), ascorbic acid, fluorescein, 1-anilino-8-naphthalensulphonic acid ammonium salt (ANS) and bovine serum albumin (BSA) were purchased from Sigma (USA) and have been used without further purification.

### 2.1. Production of fluorescent Au-clusters

Condensation of gold atoms into Au-clusters in the presence of protein (albumin) was undertaken according to [14] but using a few changes. In essence, an aqueous solution of chloroauric acid was added to the BSA protein solution in water, followed by the dropwise addition of a reducing agent, ascorbic acid, to trigger the formation of Au-clusters within the protein surface. The pH of the reaction was 11.7. In the original protocol [14] the incubation time for obtaining fluorescent Au-clusters/protein was 6 h at 37 °C. In our modified protocol we employed microwave irradiation of the reactive solution for <30 s in a microwave cavity (GE Compact Microwave Model: JES735BF, frequency 2.45 GHz, power 700 W). The microwave irradiation power was reduced to 20%, which corresponded to 140 W over the entire cavity. Microwave irradiation effectively accelerates the formation of Au-clusters within the protein structure.

### 2.2. Preparation of 'Fire in the Hole' (FIH) silver-coated plates

Silver coating of Perkin Elmer plate wells was undertaken using a protocol described previously [15]. In short, to prepare the silvering solution, 200  $\mu\text{l}$  of sodium hydroxide solution (0.5% w/v) is added to 60 ml of  $\text{AgNO}_3$  (0.83% w/v), the solution becomes brown and cloudy, after which 2 ml of ammonium hydroxide (30% solution) is added, or until the solution becomes clear. The solution is then cooled down on ice to 10 °C and, while stirring, 15 ml of fresh D-glucose solution (4.8% w/v) is added.

The silvering solution is then loaded into preheated (40 °C) plate wells for 2 min followed by cooling on ice for several minutes. The solution within the wells is changed several times, followed by continuous heating of the wells for several minutes. Finally, the plate is then washed several times with deionized water and dried in a stream of nitrogen gas.

### 2.3. Preparation of fluorescent solution of organic dyes (fluorescein and ANS)

To prepare highly fluorescent ANS/BSA complex in solution, concentrated solution of ANS was titrated into the solution of bovine serum albumin (BSA) in PBS at pH 7.4. The final concentration of BSA was 1 mg/ml ( $1.5 \times 10^{-5}$  M), the concentration of ANS was  $3 \times 10^{-5}$  M. In this condition most of ANS dye molecules are bound to the protein [16]. The BSA concentration was calculated using molar extinction coefficient  $\epsilon_{280} = 43\,600 \text{ M}^{-1} \text{ cm}^{-1}$  [16].

The concentration of fluorescein in TE buffer, pH 7.6 was  $1 \times 10^{-5}$  M. The molar extinction coefficient  $\epsilon_{490} = 80\,000 \text{ M}^{-1} \text{ cm}^{-1}$  was used for calculation the fluorescein concentration.

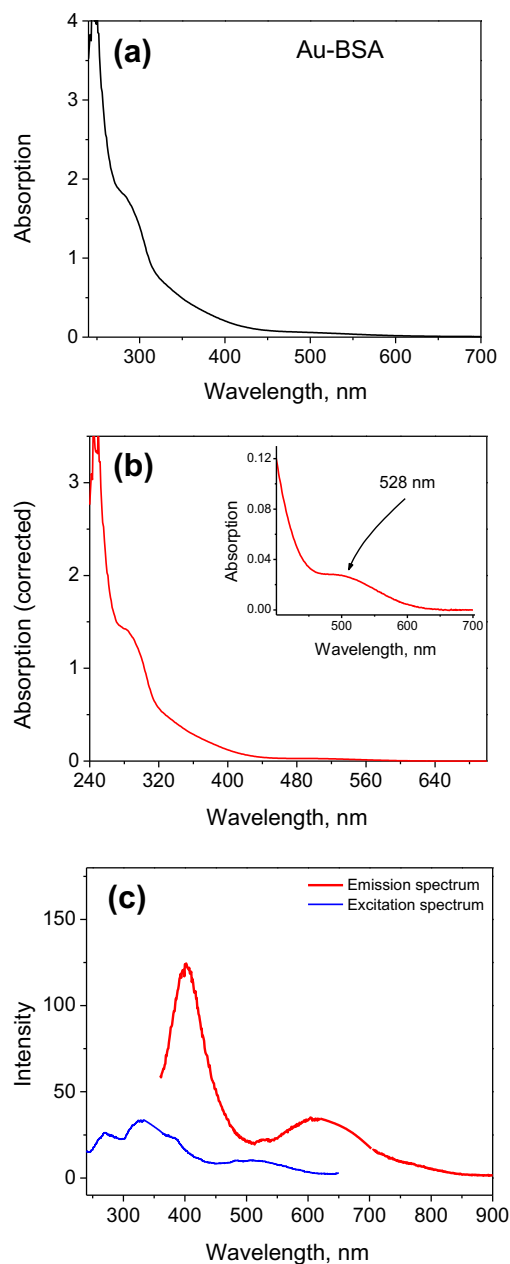


**Figure 1.** (a) Absorption spectra of Au–albumin solution. Sample was diluted 10-fold with PBS. (b) Corrected for scattering, the absorption spectrum of Au–albumin solution. Insert: enlarged absorption spectrum of Au-clusters shows specific absorption band at 528 nm. (c) Fluorescence and excitation spectra of Au-clusters (8- and 25-atoms). Fluorescence excitation spectrum was recorded using the 652 nm emission wavelength, i.e. maximum of Au–albumin fluorescence. Fluorescence spectra was recorded using the excitation wavelength at 340 nm.

### 2.4. Fluorescence measurements

Measurements of fluorescence excitation and emission spectra of the Au-protein samples were undertaken using a FluoroMax-4 spectrofluorometer (Horiba, USA).

### 2.5. Synchronous spectra measurements

Synchronous spectra of silver nanoparticle coated wells, i.e. FIH plates, were measured using a Varian spectrofluorometer plate reader. In synchronous mode the instrument measures the intensity of light from wells at different wavelengths where the wavelength of excitation and emission are equal, i.e.  $\lambda_{\text{EX}} = \lambda_{\text{EM}}$ .

### 3. Results and discussion

#### 3.1. Characterization of Au-clusters absorption and fluorescence

The absorption spectrum of the Au-cluster/protein sample is shown in Figure 1a. The spectrum consists of several overlapped spectra: Au-clusters absorption, absorption of the protein and some contribution of Rayleigh scattering. The Rayleigh scattering (RS) component of the absorption (optical density, OD) depends upon wavelength as  $OD = a/\lambda^n$ , where  $a$  and  $n$  are fitting parameters. The  $n$  parameter depends on the size of particles in solution ( $n=4$  for particles smaller than the wavelength of the scattered light). In the logarithmic form it can be written as

$$\log(OD) = \log(a) - n \times \log(\lambda). \quad (1)$$

To determine the RS contribution we have fitted the spectrum, plotted in  $\log(OD)$  vs.  $\log(\lambda)$  coordinates, to Eq. (1). It is notable that the fitted  $n$  parameter is  $n=4$ , which suggests that particles, responsible for the light scattering, are small as compared to the excitation wavelength. The obtained scattering function, Eq. (1), was subtracted from the original spectrum (Figure 1a). The result is shown in Figure 1b. Figure 1b (insert) shows that the long-wavelength absorption band has a maximum at around 528 nm, which is attributed to the absorption of condensed Au-clusters. Relatively

large gold nanoparticles (size > 5 nm), which are not fluorescent, are characterized by a plasmon resonance band positioned at about 650 nm [17].

Our Au-clusters are readily characterized by broad fluorescence and excitation spectra (Figure 1c) over the wavelength range 350–900 nm. The fluorescence spectrum consists mostly of two components: blue and red fluorescence, which is known to correspond to the emission of both 8- and 25-atom Au-clusters, respectively [18–21].

#### 3.2. Metal-enhanced fluorescence of Au-clusters

The fluorescence of Au-clusters is dramatically enhanced in silver coated plates wells, i.e. our FIH plates. Figure 2 (left) shows fluorescence and excitation spectra of a Au-cluster/protein solution recorded from silver coated and uncoated control plastic wells, Figure 2 (right). In the silvered wells both the fluorescence and excitation spectra show a large increase in intensity, relative to the control. The maximal observed MEF of Au-NCs is about  $MEF = 40$ – $50$ -fold. To the best of our knowledge this is the first observation of the MEF effect as applied to fluorescent Au-clusters.

In spectral terms, the fluorescent Au-clusters behave as classical fluorophores. They absorb and emit light, showing discrete electronic states and, accordingly, have dipoles in both the ground and excited state [21–23]. Consequently, our current model describing the origin/mechanism of the MEF effect shown in

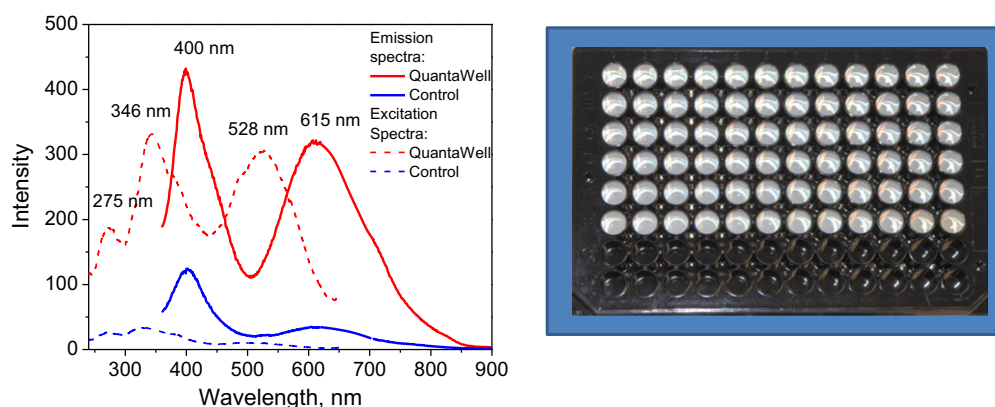


**Figure 2.** Fluorescence and excitation spectra of Au-clusters from both a FIH plate and control plastic wells (left). Real-color photograph of the 'Fire in the Hole' 96-well plate (FIH), showing both the silvered and non-silvered (control sample) wells (right). (For interpretation of the references to color in this figure legend, the reader is referred to the web version of this article.)

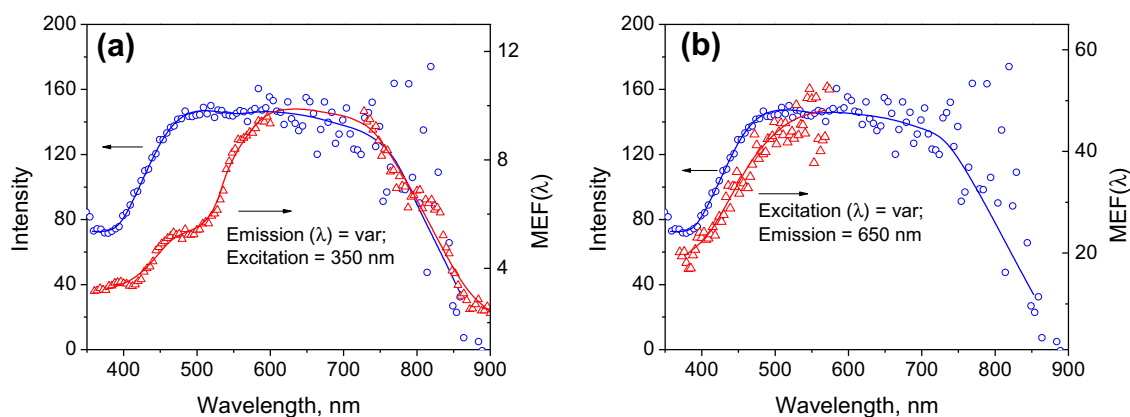


**Figure 3.** Superposition of the MEF effect and the synchronous reflection/scattering spectrum from FIH plate wells.  $MEF(\lambda)$  functions: (a) calculated as a ratio of fluorescence spectrum of Au-protein from FIH plate wells as compared to the control spectrum from an uncoated plastic well (fluorescence excitation was at 350 nm); (b) calculated as a ratio of fluorescence excitation spectra of Au-BSA from FIH plate wells to the control excitation spectrum from plastic wells (fluorescence was recorded at 650 nm).

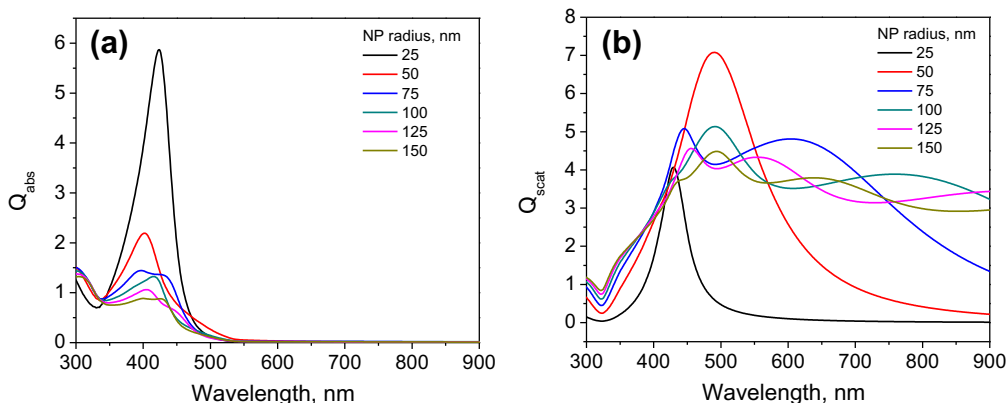


**Figure 4.** Mie calculations of the absorption (a) and scattering (b) components of the extinction spectra of silver nanoparticle. The radius of the nanoparticles changes from 25 to 150 nm in the simulations.

Figure 2 could likewise be applied to explain an enhancement of the Au-cluster fluorescence, in essence, by a coupling of the electronic system of a gold cluster with the induced surface plasmons of silver nanoparticles (NPs).

The magnitude of the observed MEF depends on both the wavelength of excitation and emission as shown in Figure 3. MEF is low (MEF = 2–4) in the UV spectral range (<400 nm), reaches maximum value (MEF = 50) in the visible range and is lower again down to MEF = 2 in the near-infrared spectral area (>750 nm).

### 3.3. Plasmon scattering from the silver surface: synchronous spectral analysis

To understand the wavelength dependence of enhancement further, we have measured the plasmon scattering spectrum from the silvered surface, and have compared it with the observed MEF spectrum. Silver particles, deposited on different surfaces (glass, quartz, various plastics), have different geometries: size, shape, density and, consequently, it is hard to simulate accurately their optical properties. Nevertheless, one can determine the general spectral properties of metal particles and their change with size. Figure 4a and b shows theoretical Mie calculations of both the absorption and scattering spectra for different size silver nanoparticles. Absorption spectra are typically narrow and their spectral position ( $\approx 400$  nm) does not change significantly, while the scattering spectrum is very sensitive to the size of the NPs becoming broad and shifting to the red when the NP size is >25 nm. For 75 nm diameter particles the scattering spectrum is quite similar to the MEF spectrum (Figure 3), i.e. covers a wavelength range from

450 to 750 nm. Subsequently, it is postulated that the scattering component of a NPs extinction spectrum can influence and modulate MEF in the broad VIS–NIR spectral region, and that this wavelength dependence can be determined from either (i) simulations or (ii) measuring the synchronous scattering spectrum, as described below.

Silver coating of our lab-made ‘Fire in the Hole’ (FIH) plate wells was specially designed to achieve a large MEF effect over a broad spectral range. We have subsequently called the technique nanopolishing [24]. The surface contains silver nanoparticles arranged on the surface in a specific multilayer manner. To characterize experimentally the spectral distribution of the plasmon scattering intensity we have recorded the synchronous spectra from the silvered surface (Figure 3). In a synchronous mode, the wavelength of excitation and emission are scanned simultaneously, which results in recording the reflection/scattering characteristic of the surface, i.e. it describes the nanoparticles’ extinction spectrum. The maximal magnitude of reflection/scattering is in the spectral range of 450–750 nm and decreases at the wavelengths <450 nm and >750 nm. It is notable that the MEF spectrum coincides very well with the synchronous scattering spectrum (Figure 3), suggesting that synchronous scatter measurements are a good predictive tool for the wavelength dependence of MEF. It is also interesting that in the 400–600 nm range, the magnitude of the MEF spectrum, estimated using the emission spectra (Figure 3a), is lower than that calculated from the fluorescence excitation spectrum (Figure 3b). We assume that this difference is a consequence of the re-absorption or energy migration between fluorescent NPs which are sited within one protein molecule. The shape of the MEF spectrum in the vis-

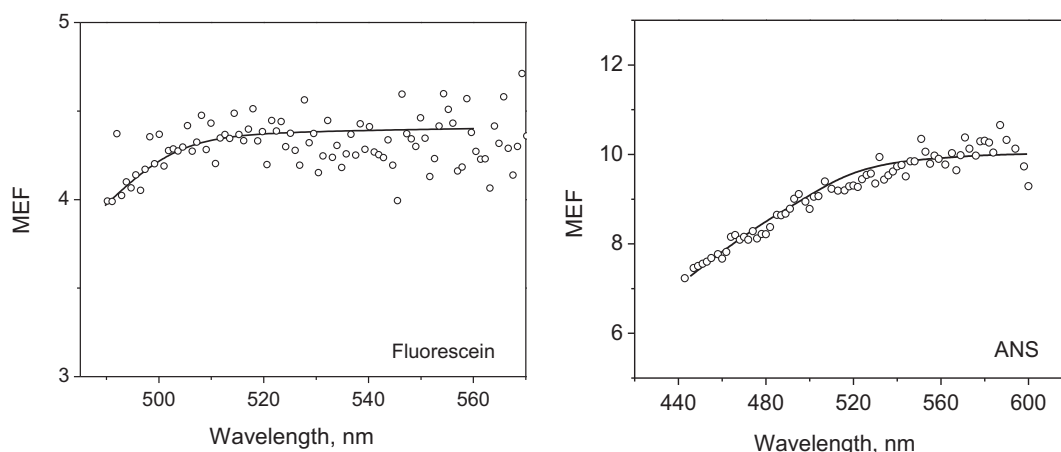


**Figure 5.** Wavelength dependence of metal-enhanced fluorescence (MEF) of fluorescein (left) and ANS, in complex with BSA, (right).

ible region, shown in Figure 3a, is a mirror-like image of Au-NCs absorption. As it can be seen from Figure 2 (left), the intense absorption band of Au(25) is positioned entirely in this spectral region, having a maximum at about 528 nm. In the case of MEF calculated using the fluorescence excitation spectra (fluorescence registration at 650 nm), the visible part of the MEF spectrum almost perfectly matches the surface scattering signature.

#### 3.4. The MEF spectrum of organic fluorophores

In contrast to Au-NCs, the fluorescence spectra of organic fluorophores are narrow. The half-width of their emission spectra is usually about 30–50 nm (e.g. the half-width of the fluorescein spectrum is  $\approx 40$  nm), which makes it complicated to analyze the MEF/plasmon scattering relationship in the broad spectral range. Among them an 1-anilino-8-naphthalen sulphonate (ANS) dye has quite broad emission spectra, half-width  $\approx 90$  nm, i.e. almost twice larger as compared to fluorescein. Nevertheless, we have analyzed the wavelength dependence of MEF for two organic fluorophores: fluorescein and ANS (ANS is fully bound to BSA). The MEF wavelength dependence for these chromophores is shown on Figure 5. Remarkably, the observed MEF spectra almost coincide with the plasmon scattering signature of silver particle surface, Figure 3.

#### 4. Conclusions

Au-clusters of 8- and 25-atom sizes, formed within a protein (BSA), have broad absorption (<600 nm) and fluorescence spectra ranging from the UV to NIR.

In the presence of close-proximity surface deposited silver nanoparticles, the fluorescence signature of the Au-NCs is enhanced dramatically (maximal MEF is >50), but in a wavelength-dependent way, i.e. observed MEF is a function of the wavelength of fluorescence registration and excitation. MEF changes from 2–4 to 50-fold, depending on wavelength.

We have shown that the MEF spectra of Au-NCs and organic dyes (fluorescein and ANS) closely match the synchronous scattering spectra. This result is in agreement with our present unified theory of metal-enhanced fluorescence [9], which explains MEF as the near-field coupling of electronic excited states to induced

surface plasmons of nanoparticles that, subsequently, radiate the photophysical characteristics of the coupled quanta.

#### Acknowledgements

The authors thank the University of Maryland, Baltimore County, and the Institute of Fluorescence for salary contributions.

#### References

- [1] J.R. Lakowicz, Principles of Fluorescence Spectroscopy, Springer Science + Business Media, LLC, New York, 2006.
- [2] B. Valeur, Molecular Fluorescence: Principles and Applications, Wiley-VCH, 2001.
- [3] S.J. Lord, N.R. Conley, H.L. Lee, R. Samuel, N. Liu, R.J. Twieg, W.E. Moerner, J. Am. Chem. Soc. 130 (2008) 9204.
- [4] K.A. Willets, O. Ostroverkhova, M. He, R.J. Twieg, W.E. Moerner, J. Am. Chem. Soc. 125 (2003) 1174.
- [5] C.D. Geddes, Metal-Enhanced Fluorescence, John Wiley & Sons, Inc., Hoboken, New Jersey, 2010.
- [6] C.D. Geddes, J.R. Lakowicz, Journal of Fluorescence 12 (2002) 121.
- [7] E.G. Matveeva, I. Gryczynski, A. Barnett, Z. Leonenko, J.R. Lakowicz, Z. Gryczynski, Anal. Biochem. 363 (2007) 239.
- [8] M. Staiano et al., ACS Appl. Mater. Interfaces 1 (2009) 2909.
- [9] K. Aslan, C.D. Geddes, Metal-enhanced fluorescence: progress towards a unified plasmon-fluorophore description, in: C.D. Geddes (Ed.), Metal-Enhanced Fluorescence, John Wiley & Sons Inc., Hoboken, New Jersey, 2010, p. 1.
- [10] A.I. Dragan, C.D. Geddes, Phys. Lett. 100 (2012) 093115.
- [11] J.R. Lakowicz, Anal. Biochem. 298 (2001) 1.
- [12] J.R. Lakowicz et al., Anal. Biochem. 301 (2002) 261.
- [13] Y. Zhang, A. Dragan, C.D. Geddes, J. Phys. Chem. C 113 (2009) 12095.
- [14] A. Retnakumari et al., Nanotechnology 21 (2010) 055103.
- [15] A.I. Dragan, M.T. Albrecht, R. Pavlovic, A.M. Keane-Myers, C.D. Geddes, Anal. Biochem. 425 (2012) 54.
- [16] D.M. Togashi, A.G. Ryder, J. Fluoresc. 18 (2008) 519.
- [17] C.I. Richards et al., J. Am. Chem. Soc. 130 (2008) 5038.
- [18] H. Kawasaki, K. Hamaguchi, I. Osaka, R. Arakawa, Adv. Funct. Mater. 21 (2011) 3508.
- [19] X. Le Guevel, B. Hotzer, G. Jung, K. Hollemeyer, V. Trouillet, M. Schneider, J. Phys. Chem. C 115 (2011) 10955.
- [20] Y. Shichibu, Y. Negishi, T. Tsukuda, T. Teranishi, J. Am. Chem. Soc. 127 (2005) 13464.
- [21] Z. Wu, R. Jin, Nano Lett. 10 (2010) 2568.
- [22] C.A. Lin et al., ACS Nano 3 (2009) 395.
- [23] O. Varnavski, G. Ramakrishna, J. Kim, D. Lee, T. Goodson, J. Am. Chem. Soc. 132 (2010) 16.
- [24] C.D. Geddes, A.I. Dragan. Enhanced luminescence from nanopolished surfaces and plate-wells, Patent pending, 2011.